2006

Search for scalar leptoquarks in the acoplanar jet topology in pp collisions at √ s = 1.96 TeV

V. M. Abazov
Joint Institute for Nuclear Research, Dubna, Russia

Kenneth A. Bloom
University of Nebraska-Lincoln, kenbloom@unl.edu

Gregory Snow
University of Nebraska-Lincoln, gsnow1@unl.edu

D0 Collaboration

Available online at www.sciencedirect.com
ScienceDirect
Physics Letters B 640 (2006) 230–237
PHYSICS LETTERS B
www.elsevier.com/locate/physletb

Search for scalar leptoquarks in the acoplanar jet topology in $p\bar{p}$ collisions at $\sqrt{s} = 1.96$ TeV

DØ Collaboration

V.M. Abazov [aj], B. Abbott [bx], M. Abolins [bn], B.S. Acharya [ac], M. Adams [az], T. Adams [ax], M. Agelou [r], J.-L. Agram [s], S.H. Ahn [ae], M. Ahsan [bh], G.D. Alexeev [aj], G. Alkhazov [an], A. Alton [bm], G. Alverson [bl], G.A. Alves [b], M. Anastasoaie [ai], T. Andeen [bb], S. Anderson [at], B. Andrieu [q], M.S. Anzelc [bb], Y. Arnoud [n], M. Arov [ba], A. Askew [ax], B. Åsman [ao], A.C.S. Assis Jesus [c], O. Atramentov [bf], C. Autermann [u], C. Avila [h], C. Ay [x], F. Badaud [m], A. Baden [bj], L. Bagby [ba], B. Baldin [ay], D.V. Bandurin [bh], P. Banerjee [ac], S. Banerjee [ac], E. Barberis [bl], P. Bargassa [cc], P. Baringer [bg], C. Barnes [ar], J. Barreto [b], J.F. Bartlett [ay], U. Bassler [q], D. Bauer [ar], A. Bean [bg], M. Begalli [c], M. Begel [bt], C. Belanger-Champagne [e], L. Bellantoni [ay], A. Bellavance [bp], J.A. Benitez [bn], S.B. Beri [aa], G. Bernardi [q], R. Bernhard [ap], L. Berntzon [o], I. Bertram [aq], M. Besançon [r], R. Beuselinck [ar], V.A. Bezzubov [am], P.C. Bhat [ay], V. Bhatnagar [aa], M. Binder [y], C. Biscarat [aq], K.M. Black [bk], I. Blackler [ar], G. Blazey [ba], F. Blekman [ar], S. Blessing [ax], D. Bloch [s], K. Bloom [bp], U. Blumenschein [w], A. Boehnlein [ay], O. Boeriu [bd], T.A. Bolton [bh], G. Borissov [aq], K. Bos [ah], T. Bose [bz], A. Brandt [ca], R. Brock [bn], G. Brooijmans [bs], A. Bross [ay], D. Brown [ca], N.J. Buchanan [ax], D. Buchholz [bb], M. Buehler [cd], V. Buescher [w], S. Burdin [ay], S. Burke [at], T.H. Burnett [ce], E. Busato [q], C.P. Buszello [ar], J.M. Butler [bk], P. Calfayan [y], S. Calvet [o], J. Cammin [bt], S. Caron [ah], W. Carvalho [c], B.C.K. Casey [bz], N.M. Cason [bd], H. Castilla-Valdez [ag], S. Chakrabarti [ac], D. Chakraborty [ba], K.M. Chan [bt], A. Chandra [aw], D. Chapin [bz], F. Charles [s], E. Cheu [at], F. Chevallier [n], D.K. Cho [bk], S. Choi [af], B. Choudhary [ab], L. Christofek [bg], D. Claes [bp], B. Clément [s], C. Clément [ao], Y. Coadou [e], M. Cooke [cc], W.E. Cooper [ay], D. Coppage [bg], M. Corcoran [cc], M.-C. Cousinou [o], B. Cox [as], S. Crépé-Renaudin [n], D. Cutts [bz], M. Ćwiok [ad], H. da Motta [b], A. Das [bk], M. Das [bi], B. Davies [aq], G. Davies [ar], G.A. Davis [bb], K. De [ca], P. de Jong [ah], S.J. de Jong [ai], E. De La Cruz-Burelo [bm], C. De Oliveira Martins [c], J.D. Degenhardt [bm], F. Déliot [r], M. Demarteau [ay], R. Demina [bt], P. Demine [r], D. Denisov [ay], S.P. Denisov [am], S. Desai [bu], H.T. Diehl [ay], M. Diesburg [ay], M. Doidge [aq], A. Dominguez [bp], H. Dong [bu], L.V. Dudko [al], L. Duflot [p], S.R. Dugad [ac], A. Duperrin [o], J. Dyer [bn], A. Dyshkant [ba], M. Eads [bp], D. Edmunds [bn], T. Edwards [as], J. Ellison [aw], J. Elmsheuser [y], V.D. Elvira [ay], S. Eno [bj], P. Ermolov [al], J. Estrada [ay], H. Evans [bc], A. Evdokimov [ak], V.N. Evdokimov [am], S.N. Fatakia [bk], L. Feligioni [bk], A.V. Ferapontov [bh], T. Ferbel [bt], F. Fiedler [y], F. Filthaut [ai], W. Fisher [ay], H.E. Fisk [ay], I. Fleck [w], M. Ford [as], M. Fortner [ba], H. Fox [w], S. Fu [ay], S. Fuess [ay], T. Gadfort [ce], C.F. Galea [ai], E. Gallas [ay], E. Galyaev [bd], C. Garcia [bt], A. Garcia-Bellido [ce], J. Gardner [bg], V. Gavrilov [ak], A. Gay [s], P. Gay [m], D. Gelé [s], R. Gelhaus [aw], C.E. Gerber [az], Y. Gershtein [ax], D. Gillberg [e], G. Ginther [bt], N. Gollub [ao], B. Gómez [h], A. Goussiou [bd], P.D. Grannis [bu], H. Greenlee [ay], Z.D. Greenwood [bi], E.M. Gregores [d], G. Grenier [t], Ph. Gris [m], J.-F. Grivaz [p,*], S. Grünendahl [ay], M.W. Grünewald [ad], F. Guo [bu], J. Guo [bu], G. Gutierrez [ay], P. Gutierrez [bx], A. Haas [bs], N.J. Hadley [bj], P. Haefner [y],

0370-2693/$ – see front matter
doi:10.1016/j.physletb.2006.08.020

S. Hagopian [ax], J. Haley [bq], I. Hall [bx], R.E. Hall [av], L. Han [g], K. Hanagaki [ay], K. Harder [bh], A. Harel [bt], R. Harrington [bl], J.M. Hauptman [bf], R. Hauser [bn], J. Hays [bb], T. Hebbeker [u], D. Hedin [ba], J.G. Hegeman [ah], J.M. Heinmiller [az], A.P. Heinson [aw], U. Heintz [bk], C. Hensel [bg], G. Hesketh [bl], M.D. Hildreth [bd], R. Hirosky [cd], J.D. Hobbs [bu], B. Hoeneisen [l], H. Hoeth [z], M. Hohlfeld [p], S.J. Hong [ae], R. Hooper [bz], P. Houben [ah], Y. Hu [bu], Z. Hubacek [j], V. Hynek [i], I. Iashvili [br], R. Illingworth [ay], A.S. Ito [ay], S. Jabeen [bk], M. Jaffré [p], S. Jain [bx], K. Jakobs [w], C. Jarvis [bj], A. Jenkins [ar], R. Jesik [ar], K. Johns [at], C. Johnson [bs], M. Johnson [ay], A. Jonckheere [ay], P. Jonsson [ar], A. Juste [ay], D. Käfer [u], S. Kahn [bv], E. Kajfasz [o], A.M. Kalinin [aj], J.M. Kalk [bi], J.R. Kalk [bn], S. Kappler [u], D. Karmanov [al], J. Kasper [bk], P. Kasper [ay], I. Katsanos [bs], D. Kau [ax], R. Kaur [aa], R. Kehoe [cb], S. Kermiche [o], S. Kesisoglou [bz], N. Khalatyan [bk], A. Khanov [by], A. Kharchilava [br], Y.M. Kharzheev [aj], D. Khatidze [bs], H. Kim [ca], T.J. Kim [ae], M.H. Kirby [ai], B. Klima [ay], J.M. Kohli [aa], J.-P. Konrath [w], M. Kopal [bx], V.M. Korablev [am], J. Kotcher [bv], B. Kothari [bs], A. Koubarovsky [al], A.V. Kozelov [am], J. Kozminski [bn,1], D. Krop [bc], A. Kryemadhi [cd], T. Kuhl [x], A. Kumar [br], S. Kunori [bj], A. Kupco [k], T. Kurča [t,2], J. Kvita [i], S. Lager [ao], S. Lammers [bs], G. Landsberg [bz], J. Lazoflores [ax], A.-C. Le Bihan [s], P. Lebrun [t], W.M. Lee [ba], A. Leflat [al], F. Lehner [ap], V. Lesne [m], J. Leveque [at], P. Lewis [ar], J. Li [ca], Q.Z. Li [ay], J.G.R. Lima [ba], D. Lincoln [ay], J. Linnemann [bn], V.V. Lipaev [am], R. Lipton [ay], Z. Liu [e], L. Lobo [ar], A. Lobodenko [an], M. Lokajicek [k], A. Lounis [s], P. Love [aq], H.J. Lubatti [ce], M. Lynker [bd], A.L. Lyon [ay], A.K.A. Maciel [b], R.J. Madaras [au], P. Mättig [z], C. Magass [u], A. Magerkurth [bm], A.-M. Magnan [n], N. Makovec [p], P.K. Mal [bd], H.B. Malbouisson [c], S. Malik [bp], V.L. Malyshev [aj], H.S. Mao [f], Y. Maravin [bh], M. Martens [ay], S.E.K. Mattingly [bz], R. McCarthy [bu], D. Meder [x], A. Melnitchouk [bo], A. Mendes [o], L. Mendoza [h], M. Merkin [al], K.W. Merritt [ay], A. Meyer [u], J. Meyer [v], M. Michaut [r], H. Miettinen [cc], T. Millet [t], J. Mitrevski [bs], J. Molina [c], N.K. Mondal [ac], J. Monk [as], R.W. Moore [e], T. Moulik [bg], G.S. Muanza [p], M. Mulders [ay], M. Mulhearn [bs], L. Mundim [c], Y.D. Mutaf [bu], E. Nagy [o], M. Naimuddin [ab], M. Narain [bk], N.A. Naumann [ai], H.A. Neal [bm], J.P. Negret [h], S. Nelson [ax], P. Neustroev [an], C. Noeding [w], A. Nomerotski [ay], S.F. Novaes [d], T. Nunnemann [y], V. O'Dell [ay], D.C. O'Neil [e], G. Obrant [an], V. Oguri [c], N. Oliveira [c], N. Oshima [ay], R. Otec [j], G.J. Otero y Garzón [az], M. Owen [as], P. Padley [cc], N. Parashar [be], S.-J. Park [bt], S.K. Park [ae], J. Parsons [bs], R. Partridge [bz], N. Parua [bu], A. Patwa [bv], G. Pawloski [cc], P.M. Perea [aw], E. Perez [r], K. Peters [as], P. Pétroff [p], M. Petteni [ar], R. Piegaia [a], M.-A. Pleier [v], P.L.M. Podesta-Lerma [ag], V.M. Podstavkov [ay], Y. Pogorelov [bd], M.-E. Pol [b], A. Pompoš [bx], B.G. Pope [bn], A.V. Popov [am], W.L. Prado da Silva [c], H.B. Prosper [ax], S. Protopopescu [bv], J. Qian [bm], A. Quadt [v], B. Quinn [bo], K.J. Rani [ac], K. Ranjan [ab], P.N. Ratoff [aq], P. Renkel [cb], S. Reucroft [bl], M. Rijssenbeek [bu], I. Ripp-Baudot [s], F. Rizatdinova [by], S. Robinson [ar], R.F. Rodrigues [c], C. Royon [r], P. Rubinov [ay], R. Ruchti [bd], V.I. Rud [al], G. Sajot [n], A. Sánchez-Hernández [ag], M.P. Sanders [bj], A. Santoro [c], G. Savage [ay], L. Sawyer [bi], T. Scanlon [ar], D. Schaile [y], R.D. Schamberger [bu], Y. Scheglov [an], H. Schellman [bb], P. Schieferdecker [y], C. Schmitt [z], C. Schwanenberger [as], A. Schwartzman [bq], R. Schwienhorst [bn], S. Sengupta [ax], H. Severini [bx], E. Shabalina [az], M. Shamim [bh], V. Shary [r], A.A. Shchukin [am], W.D. Shephard [bd], R.K. Shivpuri [ab], D. Shpakov [ay], V. Siccardi [s], R.A. Sidwell [bh], V. Simak [j], V. Sirotenko [ay], P. Skubic [bx], P. Slattery [bt], R.P. Smith [ay], G.R. Snow [bp], J. Snow [bw], S. Snyder [bv], S. Söldner-Rembold [as], X. Song [ba], L. Sonnenschein [q], A. Sopczak [aq], M. Sosebee [ca], K. Soustruznik [i], M. Souza [b], B. Spurlock [ca], J. Stark [n], J. Steele [bi], V. Stolin [ak], A. Stone [az], D.A. Stoyanova [am], J. Strandberg [ao], M.A. Strang [br], M. Strauss [bx], R. Ströhmer [y], D. Strom [bb], M. Strovink [au], L. Stutte [ay], S. Sumowidagdo [ax], A. Sznajder [c], M. Talby [o], P. Tamburello [at], W. Taylor [e], P. Telford [as], J. Temple [at], B. Tiller [y], M. Titov [w], V.V. Tokmenin [aj], M. Tomoto [ay], T. Toole [bj], I. Torchiani [w], S. Towers [aq], T. Trefzger [x], S. Trincaz-Duvoid [q], D. Tsybychev [bu], B. Tuchming [r], C. Tully [bq], A.S. Turcot [as], P.M. Tuts [bs],

R. Unalan [bn], L. Uvarov [an], S. Uvarov [an], S. Uzunyan [ba], B. Vachon [e], P.J. van den Berg [ah], R. Van Kooten [bc], W.M. van Leeuwen [ah], N. Varelas [az], E.W. Varnes [at], A. Vartapetian [ca], I.A. Vasilyev [am], M. Vaupel [z], P. Verdier [t], L.S. Vertogradov [aj], M. Verzocchi [ay], F. Villeneuve-Seguier [ar], P. Vint [ar], J.-R. Vlimant [q], E. Von Toerne [bh], M. Voutilainen [bp,3], M. Vreeswijk [ah], H.D. Wahl [ax], L. Wang [bj], J. Warchol [bd], G. Watts [ce], M. Wayne [bd], M. Weber [ay], H. Weerts [bn], N. Wermes [v], M. Wetstein [bj], A. White [ca], D. Wicke [z], G.W. Wilson [bg], S.J. Wimpenny [aw], M. Wobisch [ay], J. Womersley [ay], D.R. Wood [bl], T.R. Wyatt [as], Y. Xie [bz], N. Xuan [bd], S. Yacoob [bb], R. Yamada [ay], M. Yan [bj], T. Yasuda [ay], Y.A. Yatsunenko [aj], K. Yip [bv], H.D. Yoo [bz], S.W. Youn [bb], C. Yu [n], J. Yu [ca], A. Yurkewicz [bu], A. Zatserklyaniy [ba], C. Zeitnitz [z], D. Zhang [ay], T. Zhao [ce], B. Zhou [bm], J. Zhu [bu], M. Zielinski [bt], D. Zieminska [bc], A. Zieminski [bc], V. Zutshi [ba], E.G. Zverev [al]

[a] *Universidad de Buenos Aires, Buenos Aires, Argentina*
[b] *LAFEX, Centro Brasileiro de Pesquisas Físicas, Rio de Janeiro, Brazil*
[c] *Universidade do Estado do Rio de Janeiro, Rio de Janeiro, Brazil*
[d] *Instituto de Física Teórica, Universidade Estadual Paulista, São Paulo, Brazil*
[e] *University of Alberta, Edmonton, Alberta*
and Simon Fraser University, Burnaby, British Columbia
and York University, Toronto, Ontario
and McGill University, Montreal, Quebec, Canada
[f] *Institute of High Energy Physics, Beijing, People's Republic of China*
[g] *University of Science and Technology of China, Hefei, People's Republic of China*
[h] *Universidad de los Andes, Bogotá, Colombia*
[i] *Center for Particle Physics, Charles University, Prague, Czech Republic*
[j] *Czech Technical University, Prague, Czech Republic*
[k] *Center for Particle Physics, Institute of Physics, Academy of Sciences of the Czech Republic, Prague, Czech Republic*
[l] *Universidad San Francisco de Quito, Quito, Ecuador*
[m] *Laboratoire de Physique Corpusculaire, IN2P3-CNRS, Université Blaise Pascal, Clermont-Ferrand, France*
[n] *Laboratoire de Physique Subatomique et de Cosmologie, IN2P3-CNRS, Universite de Grenoble 1, Grenoble, France*
[o] *CPPM, IN2P3-CNRS, Université de la Méditerranée, Marseille, France*
[p] *IN2P3-CNRS, Laboratoire de l'Accélérateur Linéaire, Orsay, France*
[q] *LPNHE, IN2P3-CNRS, Universités Paris VI and VII, Paris, France*
[r] *DAPNIA/Service de Physique des Particules, CEA, Saclay, France*
[s] *IPHC, IN2P3-CNRS, Université Louis Pasteur, Strasbourg, France, and Université de Haute Alsace, Mulhouse, France*
[t] *Institut de Physique Nucléaire de Lyon, IN2P3-CNRS, Université Claude Bernard, Villeurbanne, France*
[u] *III. Physikalisches Institut A, RWTH Aachen, Aachen, Germany*
[v] *Physikalisches Institut, Universität Bonn, Bonn, Germany*
[w] *Physikalisches Institut, Universität Freiburg, Freiburg, Germany*
[x] *Institut für Physik, Universität Mainz, Mainz, Germany*
[y] *Ludwig-Maximilians-Universität München, München, Germany*
[z] *Fachbereich Physik, University of Wuppertal, Wuppertal, Germany*
[aa] *Panjab University, Chandigarh, India*
[ab] *Delhi University, Delhi, India*
[ac] *Tata Institute of Fundamental Research, Mumbai, India*
[ad] *University College Dublin, Dublin, Ireland*
[ae] *Korea Detector Laboratory, Korea University, Seoul, South Korea*
[af] *SungKyunKwan University, Suwon, South Korea*
[ag] *CINVESTAV, Mexico City, Mexico*
[ah] *FOM-Institute NIKHEF and University of Amsterdam/NIKHEF, Amsterdam, The Netherlands*
[ai] *Radboud University Nijmegen/NIKHEF, Nijmegen, The Netherlands*
[aj] *Joint Institute for Nuclear Research, Dubna, Russia*
[ak] *Institute for Theoretical and Experimental Physics, Moscow, Russia*
[al] *Moscow State University, Moscow, Russia*
[am] *Institute for High Energy Physics, Protvino, Russia*
[an] *Petersburg Nuclear Physics Institute, St. Petersburg, Russia*
[ao] *Lund University, Lund, Sweden, Royal Institute of Technology and Stockholm University, Stockholm*
and Uppsala University, Uppsala, Sweden
[ap] *Physik Institut der Universität Zürich, Zürich, Switzerland*
[aq] *Lancaster University, Lancaster, United Kingdom*
[ar] *Imperial College, London, United Kingdom*
[as] *University of Manchester, Manchester, United Kingdom*
[at] *University of Arizona, Tucson, AZ 85721, USA*
[au] *Lawrence Berkeley National Laboratory and University of California, Berkeley, CA 94720, USA*
[av] *California State University, Fresno, CA 93740, USA*

[aw] University of California, Riverside, CA 92521, USA
[ax] Florida State University, Tallahassee, FL 32306, USA
[ay] Fermi National Accelerator Laboratory, Batavia, IL 60510, USA
[az] University of Illinois at Chicago, Chicago, IL 60607, USA
[ba] Northern Illinois University, DeKalb, IL 60115, USA
[bb] Northwestern University, Evanston, IL 60208, USA
[bc] Indiana University, Bloomington, IN 47405, USA
[bd] University of Notre Dame, Notre Dame, IN 46556, USA
[be] Purdue University Calumet, Hammond, IN 46323, USA
[bf] Iowa State University, Ames, IA 50011, USA
[bg] University of Kansas, Lawrence, KS 66045, USA
[bh] Kansas State University, Manhattan, KS 66506, USA
[bi] Louisiana Tech University, Ruston, LA 71272, USA
[bj] University of Maryland, College Park, MD 20742, USA
[bk] Boston University, Boston, MA 02215, USA
[bl] Northeastern University, Boston, MA 02115, USA
[bm] University of Michigan, Ann Arbor, MI 48109, USA
[bn] Michigan State University, East Lansing, MI 48824, USA
[bo] University of Mississippi, University, MS 38677, USA
[bp] University of Nebraska, Lincoln, NE 68588, USA
[bq] Princeton University, Princeton, NJ 08544, USA
[br] State University of New York, Buffalo, NY 14260, USA
[bs] Columbia University, New York, NY 10027, USA
[bt] University of Rochester, Rochester, NY 14627, USA
[bu] State University of New York, Stony Brook, NY 11794, USA
[bv] Brookhaven National Laboratory, Upton, NY 11973, USA
[bw] Langston University, Langston, OK 73050, USA
[bx] University of Oklahoma, Norman, OK 73019, USA
[by] Oklahoma State University, Stillwater, OK 74078, USA
[bz] Brown University, Providence, RI 02912, USA
[ca] University of Texas, Arlington, TX 76019, USA
[cb] Southern Methodist University, Dallas, TX 75275, USA
[cc] Rice University, Houston, TX 77005, USA
[cd] University of Virginia, Charlottesville, VA 22901, USA
[ce] University of Washington, Seattle, WA 98195, USA

Received 7 July 2006; received in revised form 2 August 2006; accepted 11 August 2006

Available online 22 August 2006

Editor: L. Rolandi

Abstract

A search for leptoquarks has been performed in 310 pb^{-1} of data from $p\bar{p}$ collisions at a center-of-mass energy of 1.96 TeV, collected by the D0 detector at the Fermilab Tevatron Collider. The topology analyzed consists of acoplanar jets with missing transverse energy. The data show good agreement with standard model expectations, and a lower mass limit of 136 GeV has been set at the 95% C.L. for a scalar leptoquark decaying exclusively into a quark and a neutrino.

PACS: 14.80.-j; 13.85.Rm

Many extensions of the standard model (SM) that attempt to explain the apparent symmetry between quarks and leptons predict the existence of leptoquarks (LQ) [1]. These new particles are scalar or vector bosons that carry the quantum numbers of a quark–lepton system. They are expected to decay into a quark and a charged lepton with a branching fraction β, or into a quark and a neutrino with a branching fraction $(1-\beta)$. At $p\bar{p}$ colliders, leptoquarks can be pair produced, if sufficiently light, primarily by $q\bar{q}$ annihilation and gluon–gluon fusion, with a production cross section independent of the unknown leptoquark–quark–lepton coupling. For $\beta = 0$, the resulting final state consists of a pair of acoplanar quark jets with missing transverse energy, $\not\!\!E_T$, carried away by the two neutrinos.

In this Letter, a search for leptoquarks that decay into a quark and a neutrino, using data collected at a center-of-mass energy of 1.96 TeV with the D0 detector during Run II of the

* Corresponding author.
E-mail address: grivaz@lal.in2p3.fr (J.-F. Grivaz).
[1] Visitor from Lewis University, Romeoville, IL, USA.
[2] On leave from IEPSAS Kosice, Slovakia.
[3] Visitor from Helsinki Institute of Physics, Helsinki, Finland.

Fermilab Tevatron Collider, is reported. The production cross section for vector leptoquark pairs is larger than that for scalar leptoquarks, but it is model dependent. The interpretation of the results is therefore presented in terms of scalar leptoquark masses. The most constraining 95% C.L. lower mass limit for $\beta = 0$, previous to this search, was 117 GeV, obtained by the CDF Collaboration with 191 pb^{-1} of Run II data [2].

A detailed description of the D0 detector can be found in Ref. [3]. The central tracking system consists of a silicon microstrip tracker and a fiber tracker, both located within a 2 T superconducting solenoidal magnet. A liquid-argon and uranium calorimeter covers pseudorapidities up to $|\eta| \approx 4.2$, where $\eta = -\ln[\tan(\theta/2)]$ and θ is the polar angle with respect to the proton beam direction. The calorimeter consists of three sections housed in separate cryostats: the central one covers $|\eta| \lesssim 1.1$, and the two end sections extend the coverage to larger $|\eta|$. The calorimeter is segmented in depth, with four electromagnetic layers followed by up to five hadronic layers. It is also segmented in projective towers of size 0.1×0.1 in η–ϕ space, where ϕ is the azimuthal angle in radians. Calorimeter cells are formed by the intersections of towers and layers. Additional energy sampling is provided by scintillating tiles between cryostats. An outer muon system, covering $|\eta| < 2$, consists of a layer of tracking detectors and scintillation trigger counters in front of 1.8 T iron toroids, followed by two similar layers beyond the toroids.

For this search, data collected with a jets $+\not\!\!E_T$ trigger have been analyzed. At the first level, this trigger selects events in which at least three calorimeter trigger towers of size $\Delta\phi \times \Delta\eta = 0.2 \times 0.2$ record a transverse energy in excess of 5 GeV. At the second and third trigger levels, requirements are placed on $\not\!\!H_T$, the vector sum of the jet transverse momenta ($\not\!\!H_T = |\sum_{\text{jets}} \vec{p}_T|$). Coarse jets are reconstructed from trigger towers at the second level, while the full detector information is used at the third level. The $\not\!\!H_T$ thresholds are 20 and 30 GeV at the second and third levels, respectively. The trigger efficiency is larger than 98% for events fulfilling the selection criteria of this analysis. Data quality requirements on the performance of each detector subsystem yielded an available integrated luminosity of 310 pb^{-1}.

The offline analysis utilized jets reconstructed with the iterative midpoint cone algorithm [4] with a cone size of 0.5. The jet energy calibration was derived from the transverse momentum balance in photon + jet events. Only jets with $p_T > 15$ GeV that passed general quality criteria, based on the jet longitudinal profile in the calorimeter, were selected for this analysis. The missing transverse energy was calculated from all calorimeter cells, corrected for the energy calibration of reconstructed jets and for the momentum of reconstructed muons.

The sample of approximately 14 million events collected with the jets $+\not\!\!E_T$ trigger was reduced by requiring the following preselection criteria to be satisfied: at least two jets; $\not\!\!H_T > 40$ GeV; $\not\!\!E_T > 40$ GeV, where, in contrast to $\not\!\!H_T$, information from energy not belonging to reconstructed jets is taken into account; and $\Delta\Phi < 165°$, where $\Delta\Phi$ is the acoplanarity of the two leading jets, i.e., the two jets with the largest transverse momenta, defined as the difference between their azimuthal angles. To ensure that the selected events were well contained in the detector, the position of the interaction vertex along the beam direction was required to be within 60 cm of the detector center.

Events in which the presence of obvious calorimeter noise could be detected were rejected. The inefficiency associated with this procedure was measured using events collected at random beam crossings (zero-bias events), and events collected with an unbiased trigger and containing exactly two jets back-to-back in azimuth. At this stage, 306 937 events survived.

Signal efficiencies and SM backgrounds have been evaluated using a full GEANT [5] based simulation of events, with a Poisson average of 0.8 minimum-bias events superimposed, corresponding to the luminosity profile in the data sample analyzed. These simulated events were reconstructed in the same way as the data. The jet energies further received calibration corrections and an additional smearing to take into account residual differences between data and simulation, as determined with photon + jet events. The instrumental background due to jet energy mismeasurements in QCD multijet production was estimated directly from the data.

The SM processes expected to yield the largest background contributions are vector boson production in association with jets, among which $Z \to \nu\nu$ is irreducible. Vector boson pair production and top quark production have also been considered. All of these processes were generated with ALPGEN 1.3 [6], interfaced with PYTHIA 6.202 [7] for the simulation of initial and final state radiation and for jet hadronization. The parton distribution functions (PDFs) used were CTEQ5L [8]. The next-to-leading order (NLO) cross sections for vector boson production in association with jets were calculated with MCFM 3.4.4 [9] and the CTEQ5M PDFs.

The production of scalar leptoquarks via the processes $q\bar{q}$ or $gg \to \text{LQ}\overline{\text{LQ}}$ was simulated with PYTHIA and the CTEQ5L PDFs. The chosen leptoquark masses ranged from 80 to 140 GeV, in steps of 5 GeV. For each mass, 10 000 events were generated. The NLO leptoquark pair production cross sections were calculated using a program based on Ref. [10], with CTEQ6.1M PDFs [11]. For the mass range considered, they vary from 52.4 to 2.38 pb. These nominal values were obtained for a renormalization and factorization scale equal to the leptoquark mass.

The selection criteria for this analysis are listed in Table 1, together with the numbers of events surviving at each step and with the cumulative efficiency for a leptoquark mass of 140 GeV. The jet kinematic cuts **C1** to **C4** reject a large fraction of the SM and instrumental backgrounds. They take advantage of the central signal production and decay by requiring that $|\eta_{\text{det}}|$ be smaller than 1.5 for the two leading jets, where η_{det} is the pseudorapidity measured from the detector center. Cut **C5**, where EMF is the fraction of jet energy contained in the electromagnetic section of the calorimeter, rejects jets likely due to photons or electrons.

In cut **C6**, the total transverse energy of the charged particles emanating from the interaction vertex and associated with a jet, as measured in the tracking system, is compared to the jet transverse energy recorded in the calorimeter. The charged

Table 1
Numbers of data events selected and signal cumulative efficiencies for $m_{\mathrm{LQ}} = 140$ GeV at various stages of the analysis. The leading and subleading jets are denoted jet-1 and jet-2

Cut applied	Events left	Signal eff. (%)
Initial cuts	306 937	58.8
C1: jet-1 $p_T > 60$ GeV	206 116	48.7
C2: jet-1 $\lvert\eta_{\mathrm{det}}\rvert < 1.5$	160 323	46.8
C3: jet-2 $p_T > 50$ GeV	48 979	24.8
C4: jet-2 $\lvert\eta_{\mathrm{det}}\rvert < 1.5$	42 028	22.7
C5: jet-1 jet-2 EMF < 0.95	40 821	22.3
C6: jet-1 jet-2 CPF > 0.05	34 746	22.2
C7: exactly two jets	5 213	15.3
C8: $\not\!\!E_T > 70$ GeV	492	11.8
C9: isolated electron veto	465	11.7
C10: isolated muon veto	399	11.6
C11: isolated track veto	287	10.0
C12: $\Delta\Phi_{\mathrm{max}} - \Delta\Phi_{\mathrm{min}} < 120°$	180	9.4
C13: $\Delta\Phi_{\mathrm{max}} + \Delta\Phi_{\mathrm{min}} < 280°$	124	8.4
C14: $\not\!\!E_T > 80$ GeV	86	7.0

particle fraction CPF, i.e. the ratio of these two quantities, is expected to be close to zero either if a wrong interaction vertex was selected, in which case it is unlikely that the charged tracks truly associated with the jet will come from the selected vertex, or if the jet is a fake one, e.g. due to calorimeter noise, in which case there should be no real charged tracks associated with it. The efficiency of this jet confirmation procedure was determined using events containing two jets back-to-back in azimuth.

Cut **C7** was applied to suppress further the instrumental background, which is enriched in multijet events by the acoplanarity requirement. The efficiency of such a jet multiplicity cut is sensitive to the modeling of initial and final state radiation (ISR/FSR). To verify the simulation of these effects, $(Z \to ee) + \geqslant$2-jet events were selected in the data, and compared to a simulation by ALPGEN for the production of $(Z \to ee) + 2$-jets, with ISR/FSR jets added by PYTHIA. The two leading jets were required to fulfill criteria similar to those used in the analysis, and the numbers of events with additional jets were compared between data and simulation, as well as the p_T spectra of those jets. The small deficit observed in the simulation, located mostly at $p_T < 20$ GeV, was used to correct the signal and background simulations, and the statistical power of this test was taken as a systematic uncertainty.

After cut **C8**, the level of the instrumental background is largely reduced and is similar to the level of the SM backgrounds. The final $\not\!\!E_T$ cut value (cut **C14**) was optimized as explained below.

Cuts **C9**, **C10** and **C11**, reject a large fraction of the events originating from $W/Z +$ jet processes. In cut **C9**, an electron with $p_T > 10$ GeV is declared isolated if the calorimeter energy in a cone of radius 0.4 in η–ϕ around the electron direction does not exceed the energy contained in the electromagnetic layers inside a cone of radius 0.2 by more than 15%. In cut **C10**, a muon with $p_T > 10$ GeV is declared isolated if the calorimeter energy in a hollow cone with inner and outer radii 0.1 and 0.4 around the muon direction is smaller than 2.5 GeV, and if

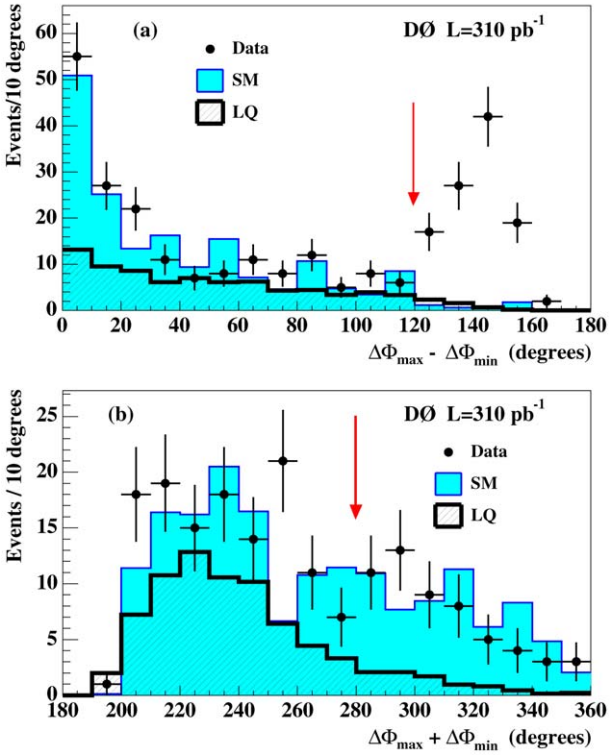

Fig. 1. Distributions of $\Delta\Phi_{\mathrm{max}} - \Delta\Phi_{\mathrm{min}}$ (a) and of $\Delta\Phi_{\mathrm{max}} + \Delta\Phi_{\mathrm{min}}$ (b) for data (points with error bars), for SM backgrounds (shaded histograms), and for a 140 GeV LQ signal (hatched histograms). In the $\Delta\Phi_{\mathrm{max}} - \Delta\Phi_{\mathrm{min}}$ distribution, cuts **C1** to **C11** are applied. The excess in data beyond 120° is attributed to the non-simulated instrumental background. In the $\Delta\Phi_{\mathrm{max}} + \Delta\Phi_{\mathrm{min}}$ distribution, the cut $\Delta\Phi_{\mathrm{max}} - \Delta\Phi_{\mathrm{min}} < 120°$ (**C12**) has been applied in addition. The locations of cuts **C12** and **C13** are indicated by arrows in (a) and (b), respectively.

the sum of the transverse energies of charged tracks, other than the muon, in a cone of radius 0.5 is smaller than 2.5 GeV. In cut **C11**, a charged track with $p_T > 5$ GeV is declared isolated if no charged track with $p_T > 0.5$ GeV is found within a hollow cone of radii 0.1 and 0.4 around the track considered. This cut was specifically designed to reject hadronic decays of τ-leptons; the use of a hollow, rather than full cone renders it efficient also in case of decays into three charged particles.

The angular correlations between the jet and $\not\!\!E_T$ directions are used to suppress both the instrumental and SM backgrounds. To this end, the minimum $\Delta\Phi_{\mathrm{min}}(\not\!\!E_T, \text{any jet})$ and maximum $\Delta\Phi_{\mathrm{max}}(\not\!\!E_T, \text{any jet})$ of the azimuthal angle differences between the $\not\!\!E_T$ direction and the direction of any of the two jets are combined as shown in Fig. 1. It can be seen in Fig. 1(a) that cut **C12** rejects most of the remaining instrumental background, which is responsible for the excess beyond 120°. Cut **C13**, which suppresses SM backgrounds at the expense of a moderate reduction of the signal efficiency, was optimized as explained below. The variable $\Delta\Phi_{\mathrm{max}} + \Delta\Phi_{\mathrm{min}}$ is the one which discriminates best the signal and the irreducible background from $(Z \to \nu\nu) + 2$-jets. Its effect is demonstrated in Fig. 1(b).

Finally, the $\not\!\!E_T$ and $\Delta\Phi_{\mathrm{max}} + \Delta\Phi_{\mathrm{min}}$ cuts were optimized for a 140 GeV LQ mass so as to minimize the cross section

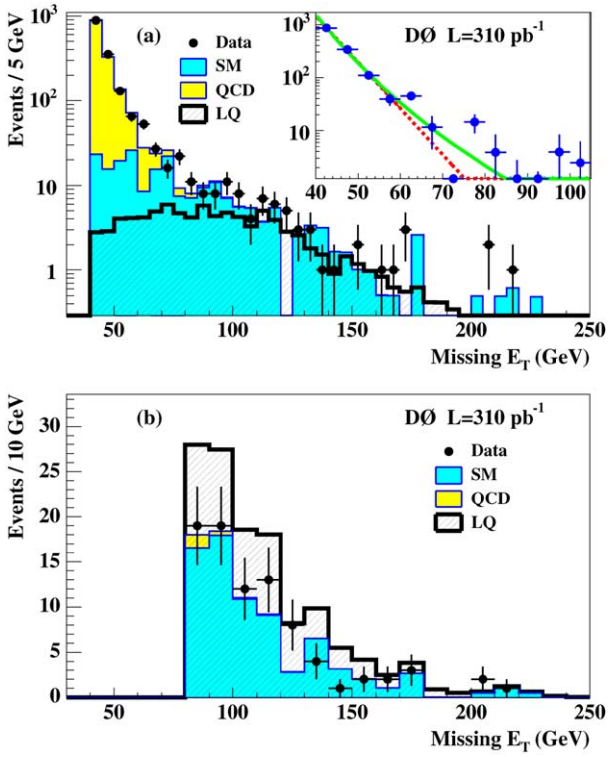

Fig. 2. Distributions of $\not\!\!E_T$ for data (points with error bars), for SM backgrounds (heavy-shaded histograms), for the instrumental background (labeled QCD, light-shaded histograms), and for a 140 GeV LQ signal. In (a), all cuts except **C8** and **C14** are applied, the LQ signal is shown as a hatched histogram, and the insert shows how the instrumental background contribution is estimated from power law (solid curve) and exponential (dashed curve) fits. The $\not\!\!E_T$ distribution in (b) is after all cuts, with the same shading code but with the signal contribution now displayed on top of all backgrounds.

expected to be excluded in the absence of signal. Cut **C8** was removed, and $\not\!\!E_T$ cut values ranging from 60 to 90 GeV were probed in 10 GeV steps. The cut on $\Delta\Phi_{\max} + \Delta\Phi_{\min}$ was varied between 260° and 300° in steps of 10°. For each set of cuts, the instrumental background was estimated as explained below. The systematic uncertainties discussed further down were taken into account in the calculation of the expected limits. The optimal set of cuts reported as **C13** and **C14** in Table 1 selects 86 data events.

The instrumental background was estimated from exponential and power law fits to the $\not\!\!E_T$ distribution (insert of Fig. 2(a)) in the range [40, 60] GeV, where the signal contribution is negligible, after subtraction of the SM expectation. Both fits were extrapolated beyond the $\not\!\!E_T$ cut value, and the average of the two results was taken as the instrumental background estimate, with a systematic uncertainty accounting for the difference between the two fit results. The final $\not\!\!E_T$ distribution is shown in Fig. 2(b). The values of the SM and instrumental backgrounds are given in Table 2. The largest background sources are, as expected, $(Z \to \nu\nu) + 2$-jets and $(W \to \ell\nu) +$ jets ($\ell = e, \mu, \tau$).

The signal efficiencies at various stages of the analysis are given in Table 1 for $m_{LQ} = 140$ GeV. The efficiency decreases together with the leptoquark mass, reaching 1.6% at 100 GeV.

Table 2
Numbers of events expected from standard model, instrumental and total backgrounds; number of data events selected; and number of signal events expected for $m_{LQ} = 140$ GeV, assuming the nominal production cross section. For the total SM and total backgrounds, as well as for the signal, the first uncertainties are statistical and the second systematic. The uncertainties on the individual SM backgrounds are statistical. The uncertainty on the instrumental background is mostly systematic from the difference between the power law and exponential fits

$(Z \to \nu\nu) + 2$-jets	34.6 ± 4.3
$(W \to \ell\nu) +$ jets	$35.0^{+9.1}_{-8.7}$
$(Z \to \ell\ell) +$ jets	$0.3^{+0.4}_{-0.2}$
$t\bar{t}$	1.9 ± 0.1
WW, WZ, ZZ	1.2 ± 0.2
Total SM background	$72.9^{+10.1\ +10.6}_{-9.7\ \ -12.1}$
Instrumental background	2.3 ± 1.2
Total background	$75.2^{+10.1\ +10.7}_{-9.7\ \ -12.2}$
Data events selected	86
Signal ($m_{\rm LQ} = 140$ GeV)	$51.8 \pm 1.8^{+5.6}_{-4.6}$

The number of signal events expected for a leptoquark mass of 140 GeV is indicated in Table 2.

The following sources of systematic uncertainty are fully correlated between SM background and signal expectations: the relative jet energy calibration between data and simulation: $^{+4}_{-8}$% for the SM background and $^{+6}_{-4}$% for the signal; the relative jet energy resolution between data and simulation: $^{+2}_{-4}$% for the SM background and negligible for the signal; the efficiency of the jet multiplicity cut: ±3%, after corrections of −3% for the SM background and −2% for the signal; the trigger efficiency: ±2% after all selection cuts; and the integrated luminosity of the analysis sample: ±6.5%.

In addition to the $^{+14}_{-13}$% statistical uncertainty of the simulation, the normalization of the SM background expectation is affected by a ±12% uncertainty, as inferred from a comparison of data and simulated $(Z \to ee) + 2$-jet events selected with the same criteria for the jets as in the analysis sample. The uncertainty of ±1.2 events on the instrumental background was estimated from power law and exponential fits to the $\not\!\!E_T$ distribution, as explained previously. As a check, the same procedure was applied to the events with $\Delta\Phi_{\max} - \Delta\Phi_{\min} > 120°$, which are dominated by the instrumental background contribution. This showed that the high $\not\!\!E_T$ tail is somewhat underestimated, possibly by as much as nine events, which leads to conservative results in terms of limit setting. Finally, the uncertainty on the signal efficiency due to the PDF choice was determined to be $^{+6}_{-4}$%, using the twenty-eigenvector basis of the CTEQ6.1M PDF set [11].

As can be seen in Table 2 and Fig. 2(b), no significant excess of events is observed in the data above the background expectation. Therefore, given the number of selected events, the SM and instrumental background expectations, the integrated luminosity of 310 pb^{-1}, the signal selection efficiency as a function of the leptoquark mass, and the statistical and systematic uncertainties discussed above, a 95% C.L. upper limit on the cross section times $(1-\beta)^2$ has been determined as shown in Fig. 3, using the modified frequentest CL_s approach [12]. The expected limit in the absence of signal is also indicated.

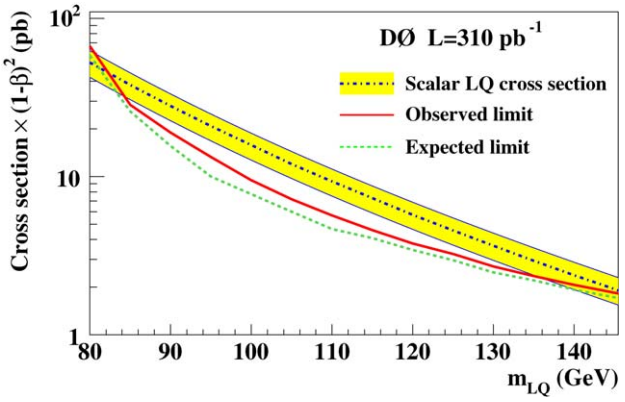

Fig. 3. Observed (solid curve) and expected (dashed curve) 95% C.L. upper limits on the cross section times $(1-\beta)^2$ as functions of the leptoquark mass. The nominal cross section for scalar-leptoquark pair production is also shown for $\beta = 0$ (dash-dotted curve), with the shaded band indicating the uncertainty due to the choices of PDFs and of renormalization and factorization scale.

The nominal theoretical cross section for the pair production of scalar leptoquarks is also shown in Fig. 3. It was obtained based on Ref. [10] with CTEQ6.1M PDFs and for a renormalization and factorization scale μ_{rf} equal to the leptoquark mass. The uncertainty associated with the PDF choice was estimated using the full set of CTEQ6.1M eigenvectors and combined quadratically with the variations obtained when μ_{rf} was modified by a factor of two up or down. For a leptoquark mass of 140 GeV, the PDF uncertainty on the theoretical cross section amounts to $^{+18}_{-13}\%$ and the scale variation results in a change of $^{+11}_{-13}\%$, the quadratic sum being $^{+21}_{-19}\%$. Reducing the nominal cross section by this theoretical uncertainty, shown as the shaded band in Fig. 3, a lower mass limit of 136 GeV is derived at the 95% C.L. Masses smaller than 85 GeV, to which this analysis is not sensitive, have been excluded previously [2, 13]. The cross section limit obtained here was combined with the results of the published D0 search for first-generation scalar leptoquarks in the $eeqq$ and $evqq$ final states [14], and the lower mass limit of 136 GeV was seen to hold independent of β.

In summary, a search for acoplanar jet final states in $p\bar{p}$ collisions at 1.96 TeV, performed using a data sample of 310 pb^{-1} collected by the D0 detector, revealed no deviation from the standard model expectation. For a single-generation scalar leptoquark, a lower mass limit of 136 GeV has been obtained for $\beta = 0$. While a tighter limit is available for third-generation leptoquarks [15], due to the increased signal purity achieved with heavy flavor tagging, this is the most stringent limit to date for first- and second-generation scalar leptoquarks decaying exclusively into a quark and a neutrino.

Acknowledgements

We thank the staffs at Fermilab and collaborating institutions, and acknowledge support from the DOE and NSF (USA); CEA and CNRS/IN2P3 (France); FASI, Rosatom and RFBR (Russia); CAPES, CNPq, FAPERJ, FAPESP and FUNDUNESP (Brazil); DAE and DST (India); Colciencias (Colombia); CONACyT (Mexico); KRF and KOSEF (Korea); CONICET and UBACyT (Argentina); FOM (The Netherlands); PPARC (United Kingdom); MSMT (Czech Republic); CRC Program, CFI, NSERC and WestGrid Project (Canada); BMBF and DFG (Germany); SFI (Ireland); The Swedish Research Council (Sweden); Research Corporation; Alexander von Humboldt Foundation; and the Marie Curie Program.

References

[1] J.C. Pati, A. Salam, Phys. Rev. D 10 (1974) 275;
H. Georgi, S. Glashow, Phys. Rev. Lett. 32 (1974) 438;
B. Schrempp, F. Schrempp, Phys. Lett. B 153 (1985) 101.
[2] D. Acosta, et al., CDF Collaboration, Phys. Rev. D 71 (2005) 112001;
D. Acosta, et al., CDF Collaboration, Phys. Rev. D 71 (2005) 119901, Erratum.
[3] V. Abazov, et al., D0 Collaboration, physics/0507191, Nucl. Instrum. Methods Phys. Res. A, in press.
[4] G.C. Blazey, et al., hep-ex/0005012.
[5] R. Brun, F. Carminati, CERN Program Library Long Writeup W5013, 1993, unpublished.
[6] M.L. Mangano, et al., JHEP 0307 (2003) 001.
[7] T. Sjöstrand, et al., Comput. Phys. Commun. 135 (2001) 238.
[8] H.L. Lai, et al., Eur. Phys. J. C 12 (2000) 375.
[9] J. Campbell, R.K. Ellis, Phys. Rev. D 60 (1999) 113006.
[10] M. Krämer, et al., Phys. Rev. Lett. 79 (1997) 341.
[11] J. Pumplin, et al., JHEP 0207 (2002) 012;
D. Stump, et al., JHEP 0310 (2003) 046.
[12] T. Junk, Nucl. Instrum. Methods Phys. Res. A 434 (1999) 435;
A. Read, in: First Workshop on Confidence Limits, CERN Report No. CERN-2000-005, 2000.
[13] D.E. Acosta, S.K. Blessing, Annu. Rev. Nucl. Part. Sci. 49 (1999) 389, and references therein.
[14] V. Abazov, et al., D0 Collaboration, Phys. Rev. D 71 (2005) 071104.
[15] T. Affolder, et al., CDF Collaboration, Phys. Rev. Lett. 85 (2000) 2056.